22p.

Technical Memorandum No. 33-153

A Study of Thermal Scale Modeling Techniques

J. M. F. Vickers

JET PROPULSION LABORATORY
CALIFORNIA INSTITUTE OF TECHNOLOGY
PASADENA, CALIFORNIA

September 30, 1963

REFERENCES

1. Uguccini, O. W. and J. H. Pollack, "A Carbon-Arc Solar Simulator," ASME paper number 62-WA-241, November 1962.
2. Clark, L. G., "Temperature Balance of Manned Space Stations," NASA TN D-1504, pp 21–31, August 1962.
3. Clark, L. G. and K. A. Laband, "Orbital Station Temperature Control," *Astronautics*, Vol. 7, No. 9, pp 40–43, September 1962.
4. Katz, A. J., "Thermal Testing," *Space/Astronautics*, Technical Reference Series, Part 2, pp 30–34, October 1962.
5. Vickers, J. M. F., Jet Propulsion Laboratory, Space Programs Summary No. 37-18, Vol. IV, pp 80–83, December 1962.
6. Jakob, M., "Heat Transfer," Vol. II, pp 6–10, John Wiley and Sons, New York, 1957.
7. Katzoff, S., "Similitude in Thermal Models of Spacecraft," NASA TN D-1631, April 1963.
8. McAdams, W. H., "Heat Transmission," Third Edition, pp 445–461, McGraw-Hill, New York, 1954.
9. Vickers, J. M. F., Jet Propulsion Laboratory, Space Programs Summary No. 37-18, Vol. IV, pp 83–85, December 1962.
10. Vickers, J. M. F., Jet Propulsion Laboratory, Space Programs Summary No. 37-19, Vol. IV, p 89, February 1963.
11. Vickers, J. M. F., Jet Propulsion Laboratory, Space Programs Summary No. 37-21, Vol. IV, pp 48–50, June 1963.

[2] (NASA Contract NAS7-100)

(NASA CR-52598; JPL-TR-33-153) OTS: $2.60ph, $0.86mf

Technical Memorandum No. 33-153

A Study of Thermal Scale Modeling Techniques

J. M. F. Vickers 30 Sep. 1963 22p n/a

R. R. McDonald

R. R. McDonald, Jr., Chief
Engineering Research Section

JET PROPULSION LABORATORY
CALIFORNIA INSTITUTE OF TECHNOLOGY
PASADENA, CALIFORNIA

September 30, 1963

Prepared Under Contract No. NAS 7-100
National Aeronautics & Space Administration

CONTENTS

TABLES

FIGURES

FIGURES (Cont'd)

ABSTRACT

11078

The techniques which may be evolved from the basic laws of thermal scale modeling for spacecraft are described. All but two of these techniques can be rejected at once, since they require conditions which are very difficult to fulfill in practice. A comparison is drawn between the two remaining techniques, the technique of preserving temperature from prototype to model and of preserving materials from prototype to model. It is found that, for steady state conditions, the technique of preserving temperature has inherent advantages over that of preserving materials, but that when transient conditions are to be modeled much of this advantage is lost.

AUTHOR

I. INTRODUCTION

The physical size of spacecraft is steadily increasing and is likely to increase further as larger boosters become available. This leads to a demand for an increase in the size of thermal test facilities. The prime cost for such facilities, including some form of solar simulation, will be considerably greater than for those presently in use. The difficulty and cost of operation will also be much greater. The type of solar simulation in the test chamber is of extreme importance, since the surface coatings are very sensitive to the spectrum of the light striking the surface. At present, the simulation system which apparently gives the best approximation to the Johnson curve for the spectral energy distribution of sunlight in space is given by carbon arcs with rare earth cores in the rods (Ref. 1). Such systems, however, are now limited to areas of good collimation of about three feet in diameter.

For these reasons it appears that thermal scale modeling will be an attractive technique when it can be developed into a working method. The use of reduced scale models will extend the useful life of test chambers already built, and will also enable the testing of still smaller scale models in conditions closely approximating actual sunlight if they can be reduced to less than three feet in diameter.

The basic laws of thermal scale modeling are well established, but experimental difficulties exist in their practical implementation. The purpose of this Report is to examine how the basic laws should be applied and what inherent advantages exist with any particular modeling basis. It will be shown that the steady state conditions (existing in interplanetary flight) have to be considered separately from the transient conditions (present during planetary encounter or midcourse maneuvers). There appears to exist a clear cut case for using a technique which preserves temperature from model to prototype in the steady state condition. The choice of the technique to be used in the transient case is not so clear, but certain recommendations are made.

II. DIMENSIONLESS GROUPS

The basic dimensionless groups for thermal scale modeling in a high vacuum, where the only heat transfer mechanisms are conduction and radiation, may be derived either from the differential equations or from consideration of the physical parameters involved. They have been stated by Clark (Ref. 2), Clark and Laband (Ref. 3) and Katz (Ref. 4), and may be conveniently written in the form used by the present author (Ref. 5) as follows:

$$\frac{\varepsilon_m \sigma T_m^3 L_m}{k_m} = \frac{\varepsilon_p \sigma T_p^3 L_p}{k_p} \quad (1)$$

$$\frac{C_m L_m}{k_m} = \frac{C_p L_p}{k_p} \quad (2)$$

$$\frac{(\rho c_p)_m L_m^2}{k_m \tau_m} = \frac{(\rho c_p)_p L_p^2}{k_p \tau_p} \quad (3)$$

$$\frac{q_m}{L_m k_m T_m} = \frac{q_p}{L_p k_p T_p} \quad (4)$$

$$\frac{q_m'' L_m}{k_m T_m} = \frac{q_p'' L_p}{k_p T_p} \quad (5)$$

$$\frac{q_m''' L_m^2}{k_m T_m} = \frac{q_p''' L_p^2}{k_p T_p} \quad (6)$$

$$\frac{\alpha_{sm} S_m L_m}{k_m T_m} = \frac{\alpha_{sp} S_p L_p}{k_p T_p} \quad (7)$$

$$\frac{\alpha_{ijm} L_m \Phi_{jim}}{k_m T_m} = \frac{\alpha_{ijp} L_p \Phi_{jip}}{k_p T_p} \quad (8)$$

Where

$$\Phi_{ji} = \frac{F_{ji} \varepsilon_j \sigma T_j^4 A_j}{A_i} \quad (9)$$

and

$$F_{ji} = \frac{1}{A_j} \int_{A_j} \int_{A_{i,v}} \frac{\cos \phi_j \cos \phi_i \, dA_i \, dA_j}{\pi r^2} \quad (10)$$

according to Jakob (Ref. 6).

Equation (1), which may be considered an analog of the Biot modulus, may be used to relate the temperatures, surface emissivities, and thermal conductivities to the scaling ratio, L_m/L_p or R. Similarly, Eq. (2) relates the joint conductances to the thermal conductivities and R. Equation (3), which is the Fourier modulus, can be used to relate the time to the thermal diffusivities and R. Equations (4), (5), and (6) can relate the net heat input, the heat flux, and the heat generated per unit volume to temperatures, thermal conductivities, and R. Finally, Eqs. (7) and (8) can be used to relate the heat flux absorbed at a surface from outside sources and that absorbed from other portions of the spacecraft to temperatures, thermal conductivities, and R. From this set of equations the basic modeling laws must now be deduced.

At first sight it would appear that within the restrictions imposed by the groupings above, a complete freedom of choice should exist in deciding the modeling laws to be followed. Katz (Ref. 4) briefly mentions some of the problems associated with two techniques, but makes no attempt to recommend either, while Clark (Ref. 2) and Clark and Laband (Ref. 3) consider only one method of attack on the problem. It is felt that these papers present only a limited discussion of the problems associated with thermal scale modeling. In the present Report, a more complete discussion is presented, together with recommendations on various modeling techniques.

III. TECHNIQUES AVAILABLE

Many modeling techniques in other areas use distorted scaling systems in which the scale ratio in one direction differs from that used in the other two. This is opposed to a geometric scale modeling system where dimensions along all three axes are reduced by the same factor. However, in all problems involving thermal radiation, it is immediately apparent that geometric scaling is vital to success since if this rule is not followed, the thermal radiation configuration factor, F_{ji}, from surface i to surface j will vary from model to prototype. While these factors can be evaluated with reasonable accuracy for simple shapes, it is extremely difficult even to estimate their values for the complex shapes involved with spacecraft. When the conditions of multiple reflectances and the variation of emissivity with direction from the normal are considered, the problem becomes impossible unless the geometry is preserved. Under these circumstances it is felt that geometric scaling of all radiating surfaces is essential to success.

The two most attractive techniques at first glance are: (1) setting the temperatures of the model and prototype the same and, (2) using the same materials for both the model and the prototype. With both of these techniques the surface emissivity would be identical for model and prototype. This comparison has been summarized by the author (Ref. 5) and the results are shown in Table 1.

An initial comparison may be drawn between the two techniques. Examination of Eqs. (5a), (7a), and (8a) shows that technique 1 involves preserving the heat flux from model to prototype. This, together with the fact that the thermal gradient is greater in the model due to the temperature preservation and the reduced geometric scale, accounts for Eq. (1a). This in turn indicates that lower conductivity materials must be used for the model. If the exact scale size is fixed by the test chamber and the prototype sizes, the thermal conductivities of all portions of the model are determined from the ratio and the thermal conductivities of the prototype materials. It is more likely, however, that the exact scale will be decided from the ratio of the thermal conductivity of the material occurring most often in the prototype to that of the most convenient modeling material which will give approximately the desired scale. This will then determine the exact conductivity ratio to be used in choosing all the other modeling materials. Katzoff (Ref. 7) suggested one method in which it is possible to produce any required thermal conductivity by cutting grooves or slots in the material (though extreme care must be taken to avoid affecting the surface properties of the material). Another method is to choose a modeling material with a thermal conductivity below that called for in the model, and then plate the surface with copper or silver. A very thin coat, a few ten-thousandths of an inch thick, will considerably modify the effective thermal conductivity without seriously affecting the geometric shape, and also without introducing any major modification of the surface geometry. A final plate or coat of paint will provide the correct surface properties. Both of these methods may lead to considerable technical problems. It appears, therefore, that the material used most commonly in the prototype should be modeled with an available material rather than a manufactured one. The combination of flux preservation and temperature preservation accounts for Eq. (2a), which indicates that the thermal contact conductance or joint conductance must be preserved from model to prototype.

Examination of Eq. (5b) shows that in technique 2 the heat flux, and, as a consequence, the temperature gradients within the structure vary as $(1/R)^{4/3}$. This means that both the heat fluxes and the temperature gradients increase rapidly as the model size is reduced. Equation (1b) shows that the absolute temperatures within the model vary as $(1/R)^{1/3}$, and will increase also as the model size is reduced. Equation (2b) indicates that the joint conductances vary as $(1/R)$, and must therefore increase as the size of the model is reduced.

Table 1. Comparison of controlling equations for model and prototype

Technique 1 Temperature and surface emissivities the same in model and prototype.		Technique 2 Materials and surface emissivities the same in model and prototype.	
$\frac{k_m}{k_p} = \frac{L_m}{L_p} = R$	(1a)	$\frac{T_m}{T_p} = \left(\frac{L_p}{L_m}\right)^{1/3} = \left(\frac{1}{R}\right)^{1/3}$	(1b)
$\frac{C_m}{C_p} = 1$	(2a)	$\frac{C_m}{C_p} = \frac{L_p}{L_m} = \frac{1}{R}$	(2b)
$\frac{\tau_m}{\tau_p} = \frac{(\rho c_p)_m L_m}{(\rho c_p)_p L_p} = \frac{(\rho c_p)_m}{(\rho c_p)_p}\left(R\right)$	(3a)	$\frac{\tau_m}{\tau_p} = \left(\frac{L_m}{L_p}\right)^2 = R^2$	(3b)
$\frac{q_m}{q_p} = \left(\frac{L_m}{L_p}\right)^2 = R^2$	(4a)	$\frac{q_m}{q_p} = \left(\frac{L_m}{L_p}\right)^{2/3} = R^{2/3}$	(4b)
$\frac{q''_m}{q''_p} = 1$	(5a)	$\frac{q''_m}{q''_p} = \left(\frac{L_p}{L_m}\right)^{4/3} = \left(\frac{1}{R}\right)^{4/3}$	(5b)
$\frac{q'''_m}{q'''_p} = \frac{L_p}{L_m} = \frac{1}{R}$	(6a)	$\frac{q'''_m}{q'''_p} = \left(\frac{L_p}{L_m}\right)^{7/3} = \left(\frac{1}{R}\right)^{7/3}$	(6b)
$\frac{\alpha_{sm} S_m}{\alpha_{sp} S_p} = 1$	(7a)	$\frac{\alpha_{sm} S_m}{\alpha_{sp} S_p} = \left(\frac{L_p}{L_m}\right)^{4/3} = \left(\frac{1}{R}\right)^{4/3}$	(7b)
$\frac{\alpha_{ijm} \Phi_{jim}}{\alpha_{ijp} \Phi_{jip}} = 1$	(8a)	$\frac{\alpha_{ijm} \Phi_{jim}}{\alpha_{ijp} \Phi_{jip}} = \left(\frac{L_p}{L_m}\right)^{4/3} = \left(\frac{1}{R}\right)^{4/3}$	(8b)

IV. STEADY STATE

A. Technique 1 (Temperature Preservation)

This first technique has an immediate advantage, since the critical item in spacecraft temperature control is the actual temperature involved. The maximum or minimum temperature to which a component is exposed is the most important criterion in deciding its performance and life so far as pure thermal behavior is concerned.

Certain inherent experimental difficulties exist with this technique, most of them associated with the variation of thermal properties with temperature. The values of the conductivity ratio between model and prototype for certain materials modeling other materials are shown in Fig. 1, over the temperature range 32°F to 572°F. In the range 32°F to 200°F, the normal range of temperatures for the major electronic components, fuels and batteries in spacecraft, the variation in the conductivity ratios for aluminum modeling copper is about 4%; for nickel modeling aluminum, about 7%; and for nickel modeling copper, about 2%. While these materials are not representative of those normally used in spacecraft, the actual values of their thermal conductivity and the variation of their thermal conductivity with temperature cover the range of values which exists for actual spacecraft materials. It should be noted, further, that the upper curve will give about 1/2 scale modeling at 70°F, the middle curve will give about 1/3 scale, and the lower curve about 1/6 scale.

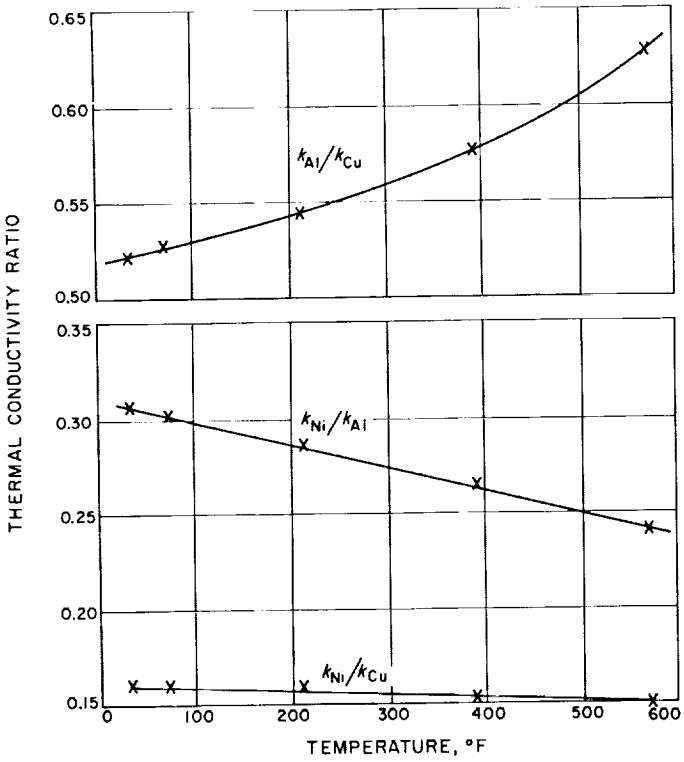

Fig. 1. Effect of temperature on thermal conductivity ratio. Values taken from McAdams (Ref. 8)

The variation in Fig. 1 shows that neither the set of Eqs. (1a) through (8a) nor the set of Eqs. (1) through (8) will actually hold, since the assumption of constant thermal properties with temperature is inherent to their derivation. It will be shown later, however, that this variation is not serious and the effect on model temperatures is small in the range of temperatures normally encountered in spacecraft.

The effect of the variation of thermal properties will be ignored and Eqs. (7a) and (8a) will be considered. Taking Eq. (8a), if temperature is preserved from model to prototype, emissivity is preserved, and geometric scaling is used, then it is possible to write $F_{jim} = F_{jip}$ and $\Phi_{jim} = \Phi_{jip}$. This means that $\alpha_{ijm} = \alpha_{ijp}$, or both the long wave length absorptivity and the emissivity are preserved from model to prototype. Equation (7a) must be treated for two separate cases; first, where true solar simulation is available and second, the case obtained in practice with all chambers, where either the solar intensity or the solar spectrum or both of these are not available in the chamber. For the first case Eq. (7a) reduces to $\alpha_{sm} = \alpha_{sp}$, that is, the complete surface properties are preserved from model to prototype. For the second case, Eq. (7a) indicates that $\alpha_{sm}/\alpha_{sp} = S_m/S_p$, that is, that the short wavelength absorptivities must be scaled in relation to the change in light intensity and wavelength/energy distribution. At the same time, the long wavelength absorptivity and the emissivity must be preserved from model to prototype.

Since the spectral distribution of monochromatic emissive power for ideal radiators is a direct function of the temperature of the source, it is possible that the conditions imposed by the equation relating the short wave length absorptivities can be satisfied. The maximum in the curve for sunlight occurs at a wavelength of about 0.5μ, while that for a black body below 1000°F lies beyond 3.5μ. If one had available a solar simulation source for a test chamber behaving approximately like

a black body above 10,000°F, then the peak will lie at about 1μ. Under these circumstances, it seems that suitable surface coatings can be found to satisfy the model requirements, i.e., identical long wavelength absorptivities and emissivities in model and prototype with scaled short wavelength absorptivities.

This point was not considered by Clark and Laband (Ref. 3), since they assumed the use of a source whose spectrum closely approximates that of the Sun. They assume, in effect, that they have true solar simulation, and can therefore use emissivities and absorptivities throughout their model which are identical to those of their prototype. However, when other sources are considered, the spectral behavior of these lamps is sufficiently different from that of the Sun that the scaling of the absorptivities can no longer be ignored unless the surfaces of the prototype approximate grey body behavior.

B. Technique 2 (Materials Preservation)

As already pointed out with the modeling technique involved in using the same materials for model and prototype, the absolute temperatures in the model will be equal to the product of the absolute temperatures of the prototype for the corresponding point and the inverse of the scale ratio raised to the one third power according to Eq. (1b). This means that a reduced scale model will have temperatures that are higher than those of the prototype.

From Eq. (1b) it can be calculated that the model temperatures corresponding to 70°F in the prototype for scales of 1/2, 1/4, 1/6, 1/8 and 1/10 are respectively, 207°F, 382°F, 503°F, 600°F and 682°F. These values, together with the ratios of the thermal conductivity at the corresponding temperature to the thermal conductivity at 70°F are shown in Fig. 2. When these results are considered, it is immediately obvious that the thermal conductivity is not constant for the material, and that for aluminum and nickel the error increases rapidly as the model decreases in physical size. At 1/10 scale, this error is approximately 20% and 12% respectively. This means that, as with technique 1, neither the special Eqs. (1b) through (8b) nor the general Eqs. (1) through (8) will apply. The corresponding temperatures and the errors in thermal conductivity ratio assuming that the thermal conductivity is constant are shown in Table 2. It will be noted that the percentage error for aluminum in the prototype is −0.2 at 32°F and 1.2 at 200°F, giving a range of percentage error of 1.4, while the range for a 1/10 scale model of aluminum for the corresponding temperatures is from 14.8 to 33.5, or a range of error of 18.7. On the other hand, for a copper prototype and model, the range decreases from 5.8 in the prototype to 1.9 in the 1/10 scale model and for nickel from 5.3 in the prototype to 3.4 in the model. The percentage error is based on the thermal conductivity at 70°F for the prototype and for the model on the thermal conductivity at the model temperature equivalent to 70°F in the prototype. It will be demonstrated later that the effect of this variation of thermal conductivity is far more serious with this technique than it was with technique 1.

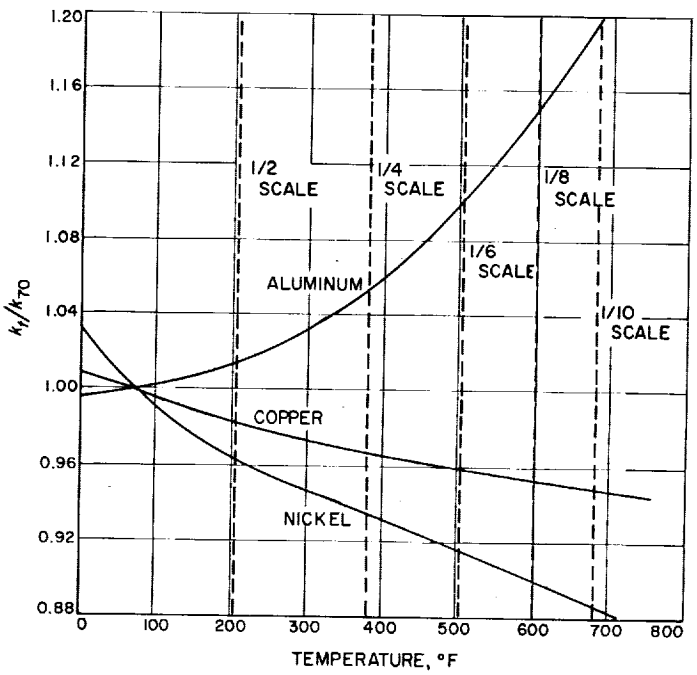

Fig. 2. Thermal conductivity ratios for aluminum, copper, and nickel

Even if the change of properties with temperature is neglected, which may be legitimate for the half scale model where the errors in assuming $k_m = k_p$ are small (Table 2), the use of Eqs. (7b) and (8b) present difficulties. When the values of Φ_{ji} from Eq. (9) are substituted in Eq. (8b) this reduces, as with technique 1, to $\alpha_{ijm}/\alpha_{ijp} = 1$. However, from Eq. (7b), with true solar simulation, the short wavelength absorptivity must be scaled according to

$$\frac{\alpha_{sm}}{\alpha_{sp}} = \left(\frac{L_p}{L_m}\right)^{4/3} \tag{11}$$

This means that the emissivity and the low temperature absorptivity must be preserved from model to prototype,

V. OTHER TECHNIQUES

Considering the number of basic parameters and equations which are available, it seems that there should be many modeling techniques that could be used. However, more detailed analysis reveals that this is not so.

If the surface treatment is assumed constant, i.e., if the emissivities and absorptivities are retained (technique 3), then for true solar simulation this reduces to technique 1. Without true solar simulation the equations become Eqs. (1c) through (8c), Table 3. This is potentially a useful system, since if S_m/S_p is less than 1, which can always be arranged, then T_m is less than T_p. This would have many advantages over technique 2 where T_m was greater than T_p with many inherent experimental problems.

Table 3. Technique 3. Surface treatment same for model and prototype

$$\frac{T_m}{T_p} = \left(\frac{S_m}{S_p}\right)^{1/4} \quad (1c)^\dagger$$

$$\frac{C_m}{C_p} = \left(\frac{S_m}{S_p}\right)^{3/4} \quad (2c)$$

$$\frac{\tau_m}{\tau_p} = \left(\frac{(\rho c_p)_m}{(\rho c_p)_p}\right)\left(\frac{L_m}{L_p}\right)\left(\frac{S_p}{S_m}\right)^{3/4} \quad (3c)$$

$$\frac{q_m}{q_p} = \left(\frac{L_m}{L_p}\right)^2 \left(\frac{S_m}{S_p}\right) \quad (4c)$$

$$\frac{q''_m}{q''_p} = \frac{S_m}{S_p} \quad (5c)$$

$$\frac{q'''_m}{q'''_p} = \left(\frac{L_p}{L_m}\right)\left(\frac{S_m}{S_p}\right) \quad (6c)$$

$$\frac{k_m}{k_p} = \left(\frac{L_m}{L_p}\right)\left(\frac{S_m}{S_p}\right)^{3/4} \quad (7c)$$

$$\frac{T_m}{T_p} = \left(\frac{S_m}{S_p}\right)^{1/4} \quad (8c)^\dagger$$

†Note that Eqs. (1) and (8) yield Eqs. (1c) and (8c) which are identical.

The following systems will not be listed as techniques since a single group eliminates them from practical use in each case.

A. System 1

If the absorptivities as well as the materials are fixed, it is possible to obtain the following relationship for the emissivities:

$$\frac{\epsilon_m}{\epsilon_p} = \left(\frac{L_p}{L_m}\right)^4 \quad (12)$$

This result cannot possibly be satisfied since, for example, the emissivity of a 1/10 scale model would have to be 10,000 times that of the prototype. In practice, the emissivity range of the present spacecraft is from 0.04 to 0.93, so that any factor increasing or decreasing this range will either lead to a demand for materials with emissivities above unity, which is impossible theoretically, or with emissivities below the lowest available, which might be possible to meet in principle but cannot be attained in practice.

B. System 2

If the variation of the surface emissivity of future spacecraft should happen to be reduced so that the highest emissivity used is less than 0.5, then it would be possible to set an upper limit for the emissivity ratio of 2. If this is then assumed, together with the preservation of materials and absorptivities, then true solar simulation cannot be used and the required values for the solar simulation are given by:

$$\frac{S_m}{S_p} = \frac{1}{1.26}\left(\frac{L_p}{L_m}\right)^{4/3} \quad (13)$$

For a 1/10 scale model this gives a simulated intensity of over 17 times that of the Sun, which is excessively large, and a value for the vicinity of Venus of about 30 times that due to the Sun in the vicinity of the Earth. In general, it appears that any attempt to modify the emissivity of the model is unlikely to succeed.

Table 2. Temperatures and errors in thermal conductivity ratio

Temperature, °F			% error in k_t^* based on $(k_p)_{70}^{**}$					
	Lower	Upper	Al	Cu	Ni	Al	Cu	Ni
Prototype	32°F	200°F	−0.2	4.0	1.6	1.2	−1.8	−3.7
Scale	Temperature in model equivalent to 32°F prototype	Temperature in model equivalent to 200°F prototype	Model temperature equivalent to 32°F			Model temperature equivalent to 200°F		
			Al	Cu	Ni	Al	Cu	Ni
1/2	160	372	0.7	−1.3	−2.6	5.6	−3.3	−6.5
1/4	321	588	3.8	−3.0	−5.7	14.1	−4.8	−9.8
1/6	434	739	7.2	−3.8	−7.4	22.6	−5.2	−11.0
1/8	524	860	11.0	−4.2	−8.8	28.2	−5.9	−12.3
1/10	600	962	14.8	−4.8	−10.0	33.5	−6.7	−13.4

*k_t = thermal conductivity of prototype or model material at temperature, °F

**$(k_p)_{70}$ = thermal conductivity of prototype material at 70°F

while the high temperature absorptivity must be scaled. This is the same problem as that encountered with technique 1 without true solar simulation. If, on the other hand, true solar simulation is not available, then Eq. (7b) must be used, with the correct values of S_m/S_p. Again, the same situation arises. The high temperature absorptivity must be scaled (though differently than for the case of true solar simulation), while the low temperature absorptivity and the emissivity must be retained. Regardless of whether or not true solar simulation is available, an extensive search must be made for surfaces with the correct properties.

In summary, technique 1 involves a search for materials for the model which have the correct thermal conductivities, or the manufacture of materials with such conductivities, but the temperatures of the model the same as those of the prototype. If true solar simulation is available, the complete surface treatment of the model will be identical to that of the prototype; if solar simulation which does not correspond to the solar spectrum either in intensity or in spectral energy distribution or both is the only type available, then the short wave length absorptivities of the model must be scaled from those of the prototype. In technique 2 the identical materials are used in model and prototype, but the temperatures of the model are scaled from those of the prototype. In the case of small-scale models, this leads to a considerable increase in temperature for the model. The short wave length absorptivities of the model must be scaled from those of the prototype regardless of whether or not true solar simulation is available. Under all circumstances, for both techniques, the emissivities and long wave length absorptivities of the model and prototype are identical.

C. System 3

If the emissivity and q‴ are preserved, then:

$$\frac{T_m}{T_p} = \left(\frac{L_m}{L_p}\right)^{1/4} \tag{14}$$

$$\frac{\alpha_{sm}}{\alpha_{sp}} = \frac{L_m}{L_p} \tag{15}$$

$$\frac{k_m}{k_p} = \left(\frac{L_m}{L_p}\right)^{7/4} \tag{16}$$

This system appears to have no advantages over techniques 1 and 2; the temperature is not preserved, the thermal conductivity is scaled more radically than for technique 1, and the short wavelength absorptivity is not preserved even if good solar simulation is available.

From the above discussion, it appears that only three techniques are feasible, 1, 2 and 3. Technique 3 neither preserves temperature from prototype to model (though with suitable choice of simulation intensity, the small scale model can run at temperatures lower than the prototype), nor does it preserve materials from prototype to model. Technique 3 is only an individual system when true solar simulation is not available – otherwise it is identical to technique 1. Techniques 1 and 2 will now be examined in greater detail.

VI. COMPARISON OF TECHNIQUES 1 AND 2

There exists one basic requirement in thermal scale modeling which must be met as closely as possible. The model must predict the temperature of the prototype throughout. This means that the model must predict the heat flux through any particular part of the prototype.

In order to assess the two techniques, three simple mathematical models were analyzed, the prototype version of which is shown in Fig. 3. This prototype was chosen as the simplest geometry which would approximate a spacecraft-type temperature control problem. It consists of a source of energy and two heat paths of different thermal conductivity leading from the heat source to separate radiating surfaces operating at different temperatures. The temperatures in the system were fixed by the heat flow distribution and the radiating characteristics of the surfaces. Technique 1 was then used to design two models at 1/10 scale, the assumed behavior of the thermal conductivity with temperature being different in the two cases. Technique 2 was used to design a third model at 1/10 scale. By using the results from the technique 2 model to forecast the prototype temperatures, the results from all three models could be compared.

The radiating surfaces at the ends of the prototype are not shown in Fig. 3, but they are assumed to be 16 ft^2 and 20 ft^2 in area, with emissivities of 1.0 and 0.943 respectively. All three dimensional effects caused by the radiating surfaces are ignored since they are merely considered a convenient rejecting device. The high input power of 1,000w was used deliberately to show the effects that might appear. This power was assumed to be delivered at a plane source of zero thickness situated at the boundary between the aluminum portion, or leg, of the model on the right and the cast iron leg of the model on the left. All other external surfaces were considered adiabatic. The cross sectional areas of the legs were one ft^2.

While the materials chosen are not representative of those used in spacecraft, the thermal conductivity of aluminum is as high as, or higher than, any normal spacecraft material with the exception of the copper used in the cabling. The thermal conductivity of cast iron is comparable to that of the lowest thermal conductivity metal used on spacecraft. In addition, the thermal conductivity of aluminum increases with increase in temperature (positive slope), while the thermal conductivity of cast iron decreases (negative slope), so that both the conditions of thermal conductivity range and of thermal conductivity behavior are fulfilled here.

No particular significance should be attached to the radiating areas or their assumed emissivities. The 16 square-foot area will dissipate 65% of the input power with an emissivity of unity at about 70°F. The 20 square feet was chosen simply as the nearest round number which will dissipate with an emissivity less than unity the remaining power, at the temperature fixed by that of the right hand end of the model, and the remaining conditions specified for the model. The exact value of the emissivity was calculated for the temperature and dissipation involved for the chosen area.

No materials exist with exactly the right values of thermal conductivity for 1/10 scale modeling of either

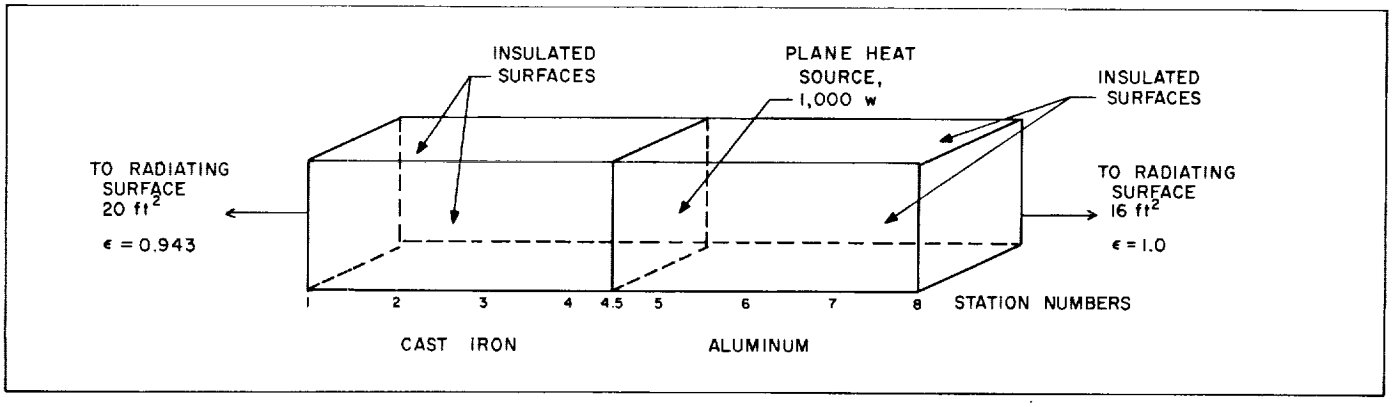

Fig. 3. Prototype

aluminum or cast iron by technique 1. Materials were assumed with the correct values of thermal conductivity, but varying with temperature twice as rapidly as do actual materials. In addition, for the first technique 1 model, it was assumed that the slopes of thermal conductivity were the reverse of those of the prototype, i.e., the material modeling the aluminum had a negative slope, while that for cast iron a positive slope. This means that the conditions assumed were worse than the worst attainable in practice. For the second model using technique 1 the slopes of thermal conductivity for the model were assumed to be the same as those of the corresponding prototype materials. For technique 2 the actual values of the thermal conductivity at the temperatures involved were used.

The results of the calculations are shown in Fig. 4 for the prototype, the technique 1 models, and for the technique 2 model. The actual technique 2 model would run at temperatures considerably above those of the prototype, however these are converted back into the corresponding figures which the model forecasts for the prototype, and it is these latter figures which are plotted in Fig. 4. The results for the second technique 1 model were indistinguishable from the prototype on this scale.

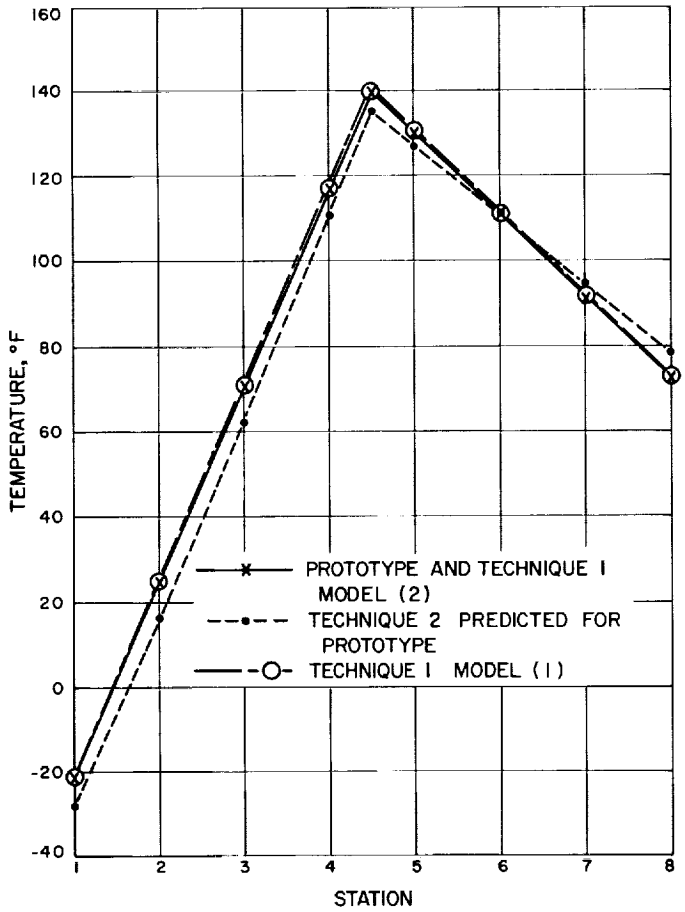

Fig. 4. Comparison of temperature and material preservation techniques

The errors involved in the two techniques can be calculated from Fig. 4 for the first model using technique 1 and the model using technique 2. The maximum errors in the absolute temperatures are 0.3% and 1.7%. While both of these are small, the difference between them is significant considering that each is inherent to its technique and will be compounded in the actual experimental work. Since all heat from a spacecraft must be dissipated finally by radiation, it is also significant to examine the error involved in T^4 if these stations were radiating instead of adiabatic. In this case the error for technique 1 is less than 1.5% while that for technique 2 is nearly 7%. For the second model using technique 1 the corresponding errors in temperature and radiant flux are 0.1% and 0.4%.

A final comparison may be drawn between the flux distributions in the left and right legs of the prototype and models. The actual ratio (right leg flux/left leg flux) is 1.857 for the prototype, 1.849 for the first technique 1 model, 1.860 for the second technique 1 model, and 2.049 for the technique 2 model. This means that the inherent errors in the flux distributions in these models are 0.43% and 0.16% for technique 1 and 10.34% for technique 2.

Considering the variety of materials already used in spacecraft, and the probability that materials with even wider ranges of behavior will be used in the future (in spacecraft where the temperature ranges are considerably larger), it was felt that the results obtained above might not be representative of certain future problems. For this reason, and in order to assess the effects of large differences in the variation of thermal conductivity with temperature, the following more extreme example was taken.

The prototype shown in Fig. 3 was assumed to be made of two materials different from those used in the earlier models, with the radiating surfaces on one square foot, the thermal conductivity of one varying with temperature from 1.0 to 0.97 and the other from 0.5 to 0.47, in a temperature range of 180°F (i.e., the thermal conductivities fell in this range by 3% and 6% respectively). The models, 1/4 scale, were assumed to be made of materials whose thermal conductivities varied in the same temperature range from 0.25 to 0.22 and 0.125 to

0.095 respectively. None of the values for the thermal conductivity have counterparts in practice, though the variation of 3% in 180°F is representative of the behavior of many materials. These variations were assumed, for the first model, to have the same slope as the prototype materials and for the second model to have the reverse slope, all thermal conductivities being in $w/(ft)^2$ °F/ft. These models differ from those described earlier. They were set up to amplify the effects of variable thermal conductivity far beyond that attained in practice in order to determine trends rather than to establish the behavior of actual materials. The results for the models are demonstrated in Fig. 5 with 10-w input to the prototype. It should be borne in mind that the results shown here are deliberately forced, the temperature drops in the two legs of each model are considerably larger than for Fig. 4, and the variation in thermal conductivity assumed for the various materials over the temperature range is very much larger than that encountered with real materials except for the right leg of the prototype. These results should not be compared with those obtained for the preservation of materials earlier, since if materials with property values varying like that of the prototype postulated here were used, the errors would be very much greater than those shown in Fig. 4. It does appear, however, that where the thermal conductivity may be expected to vary widely with temperature, such as that of nickel, a reverse sign slope is to be preferred over a slope of the same sign, since the maximum error and the mean error are considerably less under these circumstances.

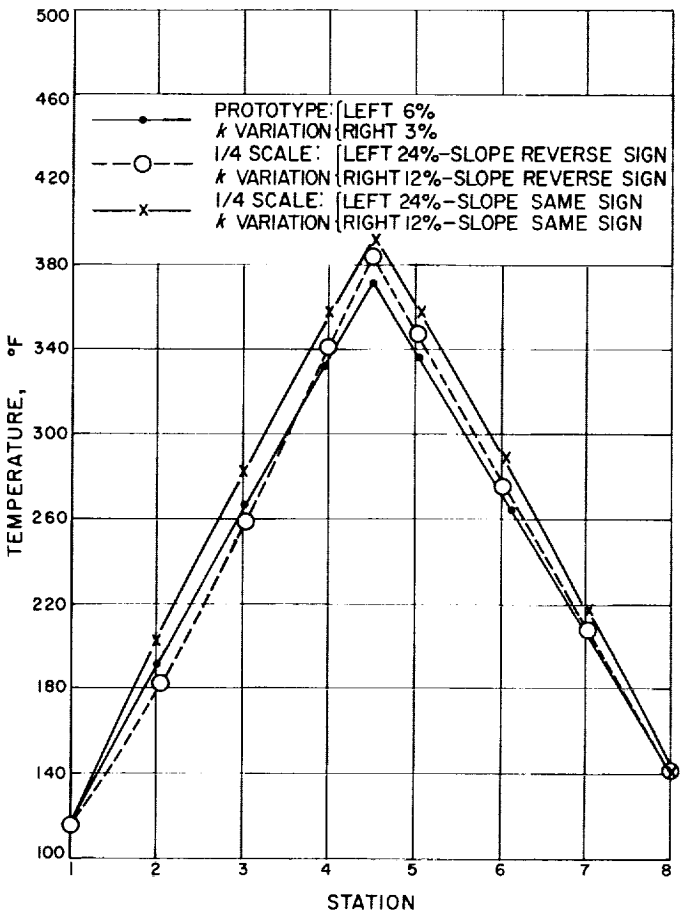

Fig. 5. Temperature distributions of prototype and models, amplified effects

VII. TRANSIENT CONDITIONS (COMPARISON OF TECHNIQUES)

Most of the life of a spacecraft is spent in interplanetary coast during which steady state heat-transfer conditions apply, or at most the extremely slow transients over periods of many days due to changes in the local value of the solar constant. However, certain transients of extreme importance do occur. They include the initial stabilization to interplanetary conditions after launch, the perturbations due to both the energy release and the change of attitude during any midcourse maneuvers which may be carried out, and the transient conditions imposed by planetary encounter. For Earth satellites or planetary orbiter vehicles the transient condition is predominant. For these reasons it is necessary to examine the laws of scale modeling for transient conditions.

If Eq. (3) is rewritten to give the time scale, it is found that the scale is dependent upon the square of the scaling ratio and the inverse of the diffusivity ratio of the model and prototype.

$$\frac{\tau_m}{\tau_p} = \frac{\alpha_p}{\alpha_m}\left(\frac{L_m}{L_p}\right)^2 \qquad (17)$$

For the case in which the variation of materials properties with temperature is ignored, the controlling dimensionless group may be derived for technique 1 from Eq. (3a) and for technique 2 from Eq. (3b).

The behaviors of the thermal diffusivity with temperature for copper, aluminum, and nickel are shown in Fig. 6. The specific behavior of these three materials should be noted, since they are representative of spacecraft materials in general. First, the diffusivity of copper decreases by about 15% in the temperature range shown; second, the diffusivity of aluminum decreases by about 6% in the first 300°F of the range, and then increases again reaching a value at 750°F which is about 1.5% above that of the value at 0°F; third, the diffusivity of nickel decreases by about 42% in the temperature range shown. These three different behaviors will be shown to have a profound effect on the modeling of transient phenomena.

The diffusivity ratios of these materials are shown in Fig. 7 over the range from 32°F to 572°F. Examination of Figs. 6 and 7 in conjunction with Eq. (17) shows that the assumptions inherent to the derivation of Eqs. (3a) and (3b) are in error, so that only the effect of the results in Eq. (17) will be considered here.

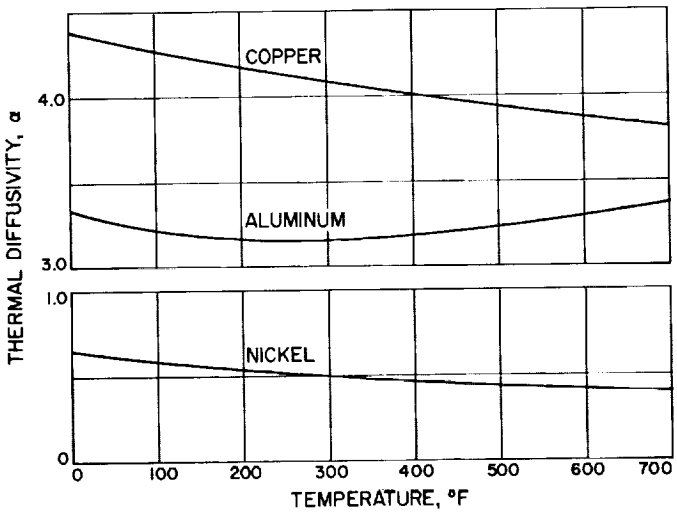

Fig. 6. The effect of temperature on the diffusivity of aluminum, copper, and nickel

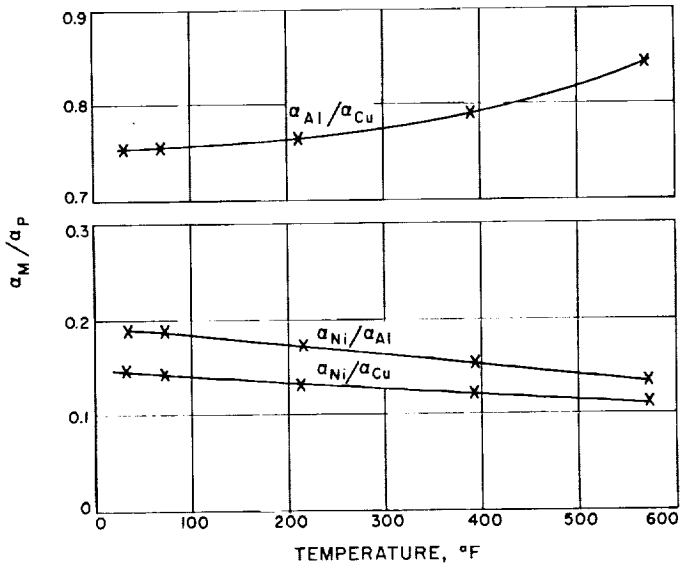

Fig. 7. The variation of diffusivity ratio with temperature for aluminum, copper, and nickel

Equation (17) shows that if the temperature varies from one portion of the model to another at any instant of time, and hence the thermal diffusivity ratio varies from point to point, then the time scale at that instant will vary from point to point in the model. In addition, during a transient, the time scale at any particular point is a function of the temperature, i.e., the time scale at

any given point will vary with the temperature-time history.

The effect of temperature on the time scale is shown in Table 4. The results for technique 1 are shown in Table 4a, the model scale being fixed by Eq. (1a) from the thermal conductivity ratio for the model and prototype at 70°F. The percentage variation over the temperature range in the scaled time is shown in Table 4c. It should be noted that the time scale variation for aluminum modeling copper is extremely small, but that for aluminum modeling nickel or nickel modeling copper is of the order of 10%.

The results for technique 2 are shown in Table 4b, and the percentage variation over the temperature range is shown in Table 4c. Here it is necessary to determine both the scaled time and the percent variation for each of the three materials to be preserved for each scale. This is because the temperature range in the model is a function of the scale ratio, Eq. (1b), and this determines the diffusivity ratio. The actual time scale is then a function of the particular diffusivity ratio and the square of the scale ratio according to Eq. (17).

Table 4c may now be used to compare the two techniques. For modeling at approximately half scale, technique 1 has a definite advantage if the behavior of the materials in question resembles that of copper and nickel. At about 1/3 scale the errors inherent with technique 1 have increased by nearly an order of magnitude, while for technique 2 they are about the same for copper and nickel and have increased by a factor of five for aluminum. This means that, if the prototype and model materials behave like copper or aluminum, there is a definite advantage at this scale in using technique 2. Finally, for about 1/6 scale, technique 1 appears to offer about the same accuracy as technique 2 using materials behaving like copper and aluminum, but has definite advantages over technique 2 using materials behaving like nickel.

One further comparison may be drawn between the two techniques. From Table 4a it can be seen that the time scale for technique 1 lies between 1/2 and 1/6, while from Table 4b the time scales for technique 2 lie between 1/4 and 1/60. This will lead to some degree of flexibility in modeling, since for the modeling of such slow transients as the time taken to reach stable conditions in interplanetary space the time scale 1/60 may reduce the test time to reasonable proportions; for such rapid transients as those involved in a midcourse maneuver it will be desirable to use a time scale at least as large as 1/2.

Table 4. Comparison of time scales for Techniques 1 and 2

a. Technique 1

Prototype	Model	Scale	Minutes in model equivalent to 1 hr in prototype	
			at 32°F	at 200°F
Copper	Aluminum	0.5280	22.15	21.80
Aluminum	Nickel	0.3013	28.65	31.25
Copper	Nickel	0.1559	10.05	10.80

b. Technique 2

Prototype and model	Minutes in model equivalent to 1 hr in prototype					
	At temperature equivalent to 32°F in prototype			At temperature equivalent to 200°F in prototype		
Scale	0.5280	0.3013	0.1559	0.5280	0.3013	0.1559
Copper	16.23	5.13	1.33	15.51	4.90	1.25
Aluminum	16.23	5.23	1.42	16.13	5.38	1.52
Nickel	15.12	4.32	1.04	12.6	3.71	0.85

c. Percent variation in model time scale from lowest model temperature to highest model temperature

Scale	Technique 1	Technique 2		
		Copper	Aluminum	Nickel
0.5280	1.6	4.4	0.6	16.7
0.3013	9.1	4.5	2.9	14.1
0.1559	7.1	6.0	7.1	18.3

VIII. CONCLUSIONS

While many modeling laws can be postulated from the dimensionless groups controlling conductive and radiative heat transfer occurring together, the actual behavior of materials and surfaces appears to prevent the use of all but two sets of these laws. Technique 1, in which the model is so designed as to have the same temperatures as the prototype, and technique 2, in which the model is designed with the same materials as the prototype.

When these two techniques are compared for steady state problems, technique 1 appears to have many advantages, whether true solar simulation is available in the test chamber or not. First, the inherent errors of technique 1 are considerably less than those encountered in technique 2, and are actually of the same order as the standard experimental errors of heat transfer. Second, if good solar simulation is available, technique 1 also involves using identical surface treatments on the model and prototype, which is considerably simpler than the absorptivity scaling called for by technique 2. Third, contact resistance, which will probably have to be simulated for some years to come, is preserved in technique 1; it has to be decreased as the model size decreases with technique 2. Fourth, it is probably more convenient to use a model in which the temperature is the same as that of the prototype, as in technique 1, than to use a model in which the temperature of the prototype must be calculated from the experimental results of the model, as in technique 2.

The problems associated with the modeling of the steady state will increase as the temperature range within a given spacecraft increases. Obviously it will be more difficult to model the solar cell array together with the rest of the spacecraft than to model either of these alone, and the introduction of nuclear reactors in spacecraft will compound the problems of modeling. However, increased temperature ranges within spacecraft will still give rise to fewer problems with technique 1 than with technique 2.

Technique 1 will lead to some difficulties in locating materials with the correct thermal conductivities, since each material in the spacecraft prototype will call for a specific thermal conductivity in the corresponding material of the model. Two approaches may be used here; first, where radiant heat exchange is insignificant and therefore the radiation configuration factor need not be preserved, the cross sectional areas of the heat conducting members may be modified rather than scaled exactly; second, where radiation is significant and the configuration factors must be preserved, the effective thermal conductivity of the path must be modified without affecting the geometric scaling. The various techniques that could be used to manufacture materials with the required thermal conductivity have been discussed.

The time scale variations within the model for transient phenomena will cause considerable difficulties, and a compromise between the relatively inaccurate temperature readings and relatively inaccurate time predictions must be sought for individual cases. Technique 1 has no overall advantage, though it appears that it will be more useful in the modeling of rapid transients. Technique 2 will be more useful in the prediction of extremely slow transients and the transition to equilibrium after launch. In general the relative behavior of the thermal diffusivities of the materials used will have to be carefully assessed for either technique. However, the transient case will be inherently more difficult to model than the steady state and since the transient times are modeled differently for different temperatures and time intervals, there will always exist errors in heat fluxes throughout the model which will then feed back causing increasing errors in the temperatures.

A contract from the Jet Propulsion Laboratory to study the feasibility of experimental thermal scale modeling has been undertaken by Arthur D. Little Incorporated of Cambridge, Massachusetts. The first phase of this contract showed that it was possible to model a fin, heated at one end and radiating to liquid nitrogen-cooled walls. The fin was divided into two sections separated by a simulated contact resistance (Refs. 9 and 10). In the second phase, a more complicated prototype is being modeled in two and three dimensional heat flow at 1/2 scale and 1/5 scale (Ref. 11). These experiments seem to indicate that the use of technique 1 provides satisfactory results. A report on this contract will be made later.

In summary, it appears that there is no inherent theoretical reason why steady state conditions cannot be successfully modeled for spacecraft. Obviously there is much to be done in developing the experimental and fabrication techniques, but no major technical breakthrough is required. The inherent errors involved with the technique recommended here are of the order of normal experimental error. The modeling of transient

conditions is less clear-cut; more compromise is required, and the inherent errors are larger due to feedback between errors in scaled time and errors in temperature. However, it appears that it will be possible to develop a reasonable technique, though the effort involved will be considerably greater than for the steady state.

NOMENCLATURE

A	area of surface
$A_{i,v}$	area of A_i which is visible from dA_j
c_p	specific heat
C	thermal contact conductance
F_{ji}	thermal radiation configuration factor from surface i to surface j
k	thermal conductivity
L	length
q	net heat input to a certain portion of the spacecraft
q''	net heat flux
q'''	internal power generated per unit volume
r	magnitude of the vector r between elemental areas dA_i and dA_j
R	scale ratio, L_m/L_p
S	radiant flux from external source
t	temperature
T	absolute temperature
α	thermal diffusivity
α_s	absorptivity of surface to external radiation spectrum
α_{ij}	absorptivity of surface i to radiation from surface j
ε	total hemispherical emissivity
ρ	density
σ	Stefan-Boltzmann constant
τ	time
ϕ	angle formed by r and the normal to the respective elemental area
Φ_{ji}	intensity of radiation from surface j incident on surface i

Subscripts:

m and p refer to model and prototype respectively

t and 70 refer to temperatures of the material in degrees fahrenheit and to the reference temperature, 70°F, respectively

Cu, Al and Ni refer to Copper, Aluminum and Nickel, respectively